

Improving the efficiency of G_0W_0 calculations with approximate spectral decompositions of dielectric matrices

Han Yang,^{1, 2} Marco Govoni,^{2, 3} and Giulia Galli^{1, 2, 3, a)}

¹⁾*Department of Chemistry, University of Chicago, Chicago, Illinois 60637, United States*

²⁾*Pritzker School of Molecular Engineering, University of Chicago, Chicago, Illinois 60637, United States*

³⁾*Materials Science Division and Center for Molecular Engineering, Argonne National Laboratory, Lemont, Illinois 60439, United States*

(Dated: 21 January 2022)

Recently it was shown that the calculation of quasiparticle energies using the G_0W_0 approximation can be performed without computing explicitly any virtual electronic states, by expanding the Green function and screened Coulomb interaction in terms of the eigenstates of the static dielectric matrix. Avoiding the evaluation of virtual electronic states leads to improved efficiency and ease of convergence of G_0W_0 calculations. Here we propose a further improvement of the efficiency of these calculations, based on an approximation of density-density response functions of molecules and solids. The approximation relies on the calculation of a subset of eigenvectors of the dielectric matrix using the kinetic operator instead of the full Hamiltonian, and it does not lead to any substantial loss of accuracy for the quasiparticle energies. The computational savings introduced by this approximation depend on the system, and they become more substantial as the number of electrons increases.

^{a)}gagalli@uchicago.edu

I. INTRODUCTION

Devising accurate and efficient methods to predict the electronic properties of molecules and condensed systems is an active field of research. Density functional theory (DFT) has been widely used for electronic structure calculations.^{1–3} However, the exact form of the exchange-correlation functional is unknown and therefore DFT results depend on the choice of approximate functionals. Improvement over DFT results may be obtained by using many-body perturbation theory (MBPT).^{4,5} A practical formulation of MBPT for many electron systems was proposed by Hedin,⁶ where the self-energy Σ is written in terms of the Green's function G and the screened Coulomb interaction W .

The GW approximation^{5,6} has been successful in the description of the electronic properties of several classes of materials and molecules;^{7–12} however the computational cost of GW calculations remains rather demanding and many complex systems cannot yet be studied using MBPT. Hence, algorithmic improvements are required to apply MBPT to realistic systems. One of the most demanding steps of the original implementation of GW calculations^{13–17} involves an explicit summation over a large number of unoccupied single particle electronic orbitals, which enter the evaluation of the dielectric matrix ϵ ^{18,19} defining the screened Coulomb interaction W ($W = \epsilon^{-1}v_c$, where v_c is the Coulomb interaction). The summation usually converges slowly as a function of the number of virtual orbitals (N_c).

In recent years, several approaches have been proposed to improve the efficiency of GW calculations. For example, in Ref. 20 it was suggested to replace unoccupied orbitals with approximate physical orbitals (SAPOs); the author of Ref. 21 simply truncated the sum over empty states entering the calculation of the irreducible density-density response function, and assigned the same, average energy to all the empty states higher than a preset value; in a

similar fashion, in Ref. 22 an integration over the density of empty states higher than a preset value was used. Other approaches adopted sophisticated algorithms to invert the dielectric matrix, e.g. in Ref. 23, they employed a Lanczos algorithm. Recently, an implementation of G_0W_0 calculations avoiding altogether explicit summations over unoccupied orbitals, as well as the necessity to invert dielectric matrices, has been proposed,^{24–28} based on the spectral decomposition of density-density response functions in terms of eigenvectors (also known as projective dielectric eigenpotentials, PDEPs). In spite of the efficiency improvement introduced by such formulation, G_0W_0 calculations for large systems remain computationally demanding.

In this paper, we propose an approximation to the projective dielectric technique,²⁴ which in many cases leads to computational savings of G_0W_0 calculations of 10-50%, without compromising accuracy. The rest of the paper is organized as follows: we describe the proposed methodology in section II and then we present results for several systems in section III, followed by our conclusions.

II. METHODOLOGY

We compute the density-density response function of solids and molecules within the framework of the random phase approximation (RPA), using projective dielectric eigenpotentials (PDEP)^{24,25,28}. The accuracy of this approach has been extensively tested for molecules and solids.²⁵ The technique relies on the solution of the Sternheimer's equation²⁹

$$(\hat{H} - \varepsilon_v \hat{I})|\Delta\psi_v\rangle = -\hat{P}_c \Delta \hat{V} |\psi_v\rangle \quad (1)$$

to obtain the linear variation of the v -th occupied electronic orbital, $|\Delta\psi_v\rangle$, induced by the external perturbation $\Delta\hat{V}$. In Eq. 1, \hat{I} is the identity operator, \hat{P}_c is the projector onto the unoccupied states, ε_v and ψ_v are the v -th eigenvalue and eigenvector of the unperturbed Kohn-Sham Hamiltonian $\hat{H} = \hat{K} + \hat{V}_{\text{SCF}}$, respectively, where $\hat{K} = -\frac{\nabla^2}{2}$ is the kinetic energy, \hat{V}_{SCF} is the self-consistent potential. For each perturbation, the first order response of the density Δn can be obtained as³⁰

$$\Delta n = 2 \sum_v \psi_v \Delta\psi_v + c.c. \quad (2)$$

Eq. 1 and 2 can be used to iteratively diagonalize the static symmetrized *irreducible* density-density response, $\tilde{\chi}_0$:^{24,25,28}

$$\tilde{\chi}_0 = \sum_{i=1}^{N_{\text{PDEP}}} |\xi_i\rangle \lambda_i \langle \xi_i|, \quad (3)$$

where λ_i and ξ_i are eigenvalues and eigenvectors of $\tilde{\chi}_0$ and N_{PDEP} is the number of eigenvectors of $\tilde{\chi}_0$, respectively. The eigenvectors ξ_i are called PDEPs: projective dielectric eigenpotentials throughout the manuscript. The symmetrized irreducible density-density response function is defined as $\tilde{\chi}_0 = v_c^{1/2} \chi_0 v_c^{1/2}$, where v_c is the Coulomb potential.²⁸ Within the RPA, the symmetrized *reducible* density-density response can be expressed as $\tilde{\chi} = (1 - \tilde{\chi}_0)^{-1} \tilde{\chi}_0$, therefore the ξ_i are also eigenvectors of $\tilde{\chi}$. The projective dielectric technique has also been recently applied beyond the RPA using a finite field method.³¹

When solving the Sternheimer's equation, it is not necessary to compute explicitly the electronic empty states, because one can write $\hat{P}_c = \hat{I} - \hat{P}_v$, since the eigenvectors of \hat{H} form a complete basis set (\hat{P}_v is the projector onto the occupied states). The use of Eq. 3 significantly reduces the cost of G_0W_0 calculation from $N_{\text{pw}}^2 N_v N_c$ to $N_{\text{PDEP}} N_{\text{pw}} N_v^2$ where N_v , N_c , N_{PDEP} , N_{pw} are numbers of occupied orbitals (valence bands in solids), virtual

orbitals (conduction bands in solids), PDEPs and plane waves, respectively, and importantly $N_{\text{PDEP}} \ll N_{\text{pw}}$.

The application of the algorithm described above to large systems is hindered by the cost of solving Eq. 1. However, we note that the eigenvalues of $\tilde{\chi}_0$ rapidly converge to zero^{,9,24,25,32} (an example is shown in Fig. 1). In addition, as shown in Ref. 25, the eigenvalue spectrum of the dielectric function for eigenvectors higher than the first few, is similar to that of the Lindhard function.³³ Hence we propose to compute the PDEPs of $\tilde{\chi}_0$ corresponding to the lowest eigenvalues using Eq. 1 and 2 and to compute the remaining ones with a less costly approach. Inspired by the work of Rocca³⁴, we approximate the eigenpotentials corresponding to higher eigenvalues with kinetic eigenpotentials, which are obtained approximating the full Hamiltonian entering Eq. 1 with the kinetic operator(\hat{K}):^{34,35}

$$(\hat{K} - \varepsilon_v \hat{I})|\Delta\psi_v\rangle = -\hat{P}_c \Delta \hat{V} |\psi_v\rangle. \quad (4)$$

In the following, we refer to the eigenpotentials from Eq. 1 as standard PDEPs (stdPDEP, ξ_i , $i = 1, \dots, N_{\text{stdPDEP}}$) and those from Eq. 4 as kinetic PDEPs (kinPDEP, η_i , $i = 1, \dots, N_{\text{kinPDEP}}$) and we rewrite the irreducible density-density response function as

$$\tilde{\chi}_0 = \sum_{i=1}^{N_{\text{stdPDEP}}} |\xi_i\rangle \lambda_i \langle \xi_i| + \sum_{j=1}^{N_{\text{kinPDEP}}} |\eta_j\rangle \mu_j \langle \eta_j|, \quad (5)$$

where ξ_i and η_j are standard and kinetic PDEPs, respectively, and λ_i and μ_j are their corresponding eigenvalues. The procedure to generate stdPDEPs and kinPDEPs is summarized in Fig. 2. We note that during the construction of kinetic PDEPs, the projection operator $\hat{P} = \hat{I} - \sum_{N_{\text{stdPDEP}}} |\xi_i\rangle \langle \xi_i|$ was applied so as to satisfy the orthonormality constrain, $\langle \xi_i | \xi_j \rangle = \delta_{ij}$, $\langle \eta_i | \eta_j \rangle = \delta_{ij}$ and $\langle \xi_i | \eta_j \rangle = 0$, $\forall(i, j)$; in addition we applied $v_c^{1/2}$ to perturbations

to yield a *symmetrized* irreducible response function $\tilde{\chi}_0$.

In our G_0W_0 calculations, both the static Green's function and the statically screened Coulomb interaction are written in the basis of eigenpotentials of the dielectric matrix. Frequency integration is performed using a contour deformation algorithm. A detailed description of the implementation of G_0W_0 calculations in the basis of eigenpotentials can be found in Ref. 26–28.

III. VALIDATION AND RESULTS

We now turn to discussing results for molecules and solids obtained by using a combination of standard and kinetic PDEPs. To examine the efficiency and applicability of the approximation proposed in section II, we performed G_0W_0 calculations for a set of closed-shell small molecules, a larger molecule (Buckminsterfullerene C₆₀), and an amorphous silicon nitride/silicon interface (Si₃N₄/Si) with a total of 1152 valence electrons. All Kohn-Sham eigenvalues and eigenvectors were obtained with the QuantumEspresso package,^{36,37} using the PBE approximation³⁸, SG15³⁹ ONCV⁴⁰ pseudopotentials and G_0W_0 calculations were carried out with the WEST code.²⁸

We first considered a subset of molecules taken from the G2/97 test set⁴¹ and calculated their vertical ionization potential (VIP) and electron affinity (EA) using different numbers of stdPDEPs (N_{stdPDEP}) and kinPDEPs (N_{kinPDEP}). We chose a plane wave cutoff of 85 Ry and a periodic box of edge 30 Bohr. For all molecules, we included either 20 or 100 stdPDEPs in our calculations, then added 100, 200, 300, 400 kinPDEPs in subsequent calculations, after which an extrapolation was performed ($a + \frac{b}{N_{\text{stdPDEP}} + N_{\text{kinPDEP}}}$) to find converged values (one example is shown in Fig. 3). These results are given in the second (A) and third columns (B) of Table I and Table II. The reference results reported in the last column (C) of the two

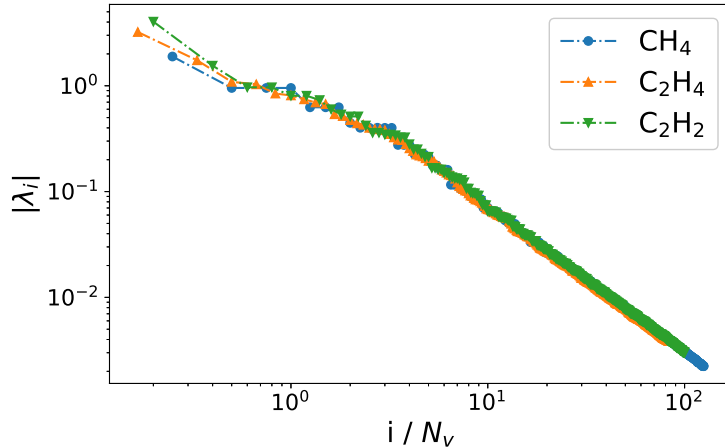


FIG. 1. First 500 eigenvalues λ_i of the symmetrized irreducible density-density response function $\tilde{\chi}_0$ (see text), for three small molecules: CH_4 (blue dots), C_2H_4 (orange up triangles), and C_2H_2 (green down triangles). N_v is the number of occupied orbitals.

tables were obtained with 200, 300, 400, 500 stdPDEPs and an extrapolation was applied. We found that including only 20 stdPDEPs yields quasiparticle energies accurate within 0.1 eV relative to the reference G_0W_0 values obtained using only standard eigenpotentials. (See also Fig. 2 of the Supplementary Information). The two data sets starting from 20 or 100 stdPDEPs enabled us to save 40% and 10% of computer time compared to the time usage needed with only standard eigenpotentials.

Table III shows our results for the C_{60} molecule. The structure of C_{60} (point group I_h) was also taken from the NIST computational chemistry database,⁴² (optimized with the $\omega\text{B}97\text{X-D}$ functional and cc-pVTZ basis sets) and no further optimization was carried out. We used the PBE exchange-correlation functional, a plane wave energy cutoff of 40 Ry and cell size of 40 bohr, the same as used in Ref. 27. We performed two groups of calculations starting with 100 and 200 standard eigenpotentials, respectively. For both calculations, we computed quasiparticle energies by adding 100, 200, 300, 400 kinetic eigenpotentials and extrapolation was done in the same manner. As seen in Table III, the results obtained with 200 standard eigenpotentials and additional kinetic eigenpotentials differ at most by 0.1 eV

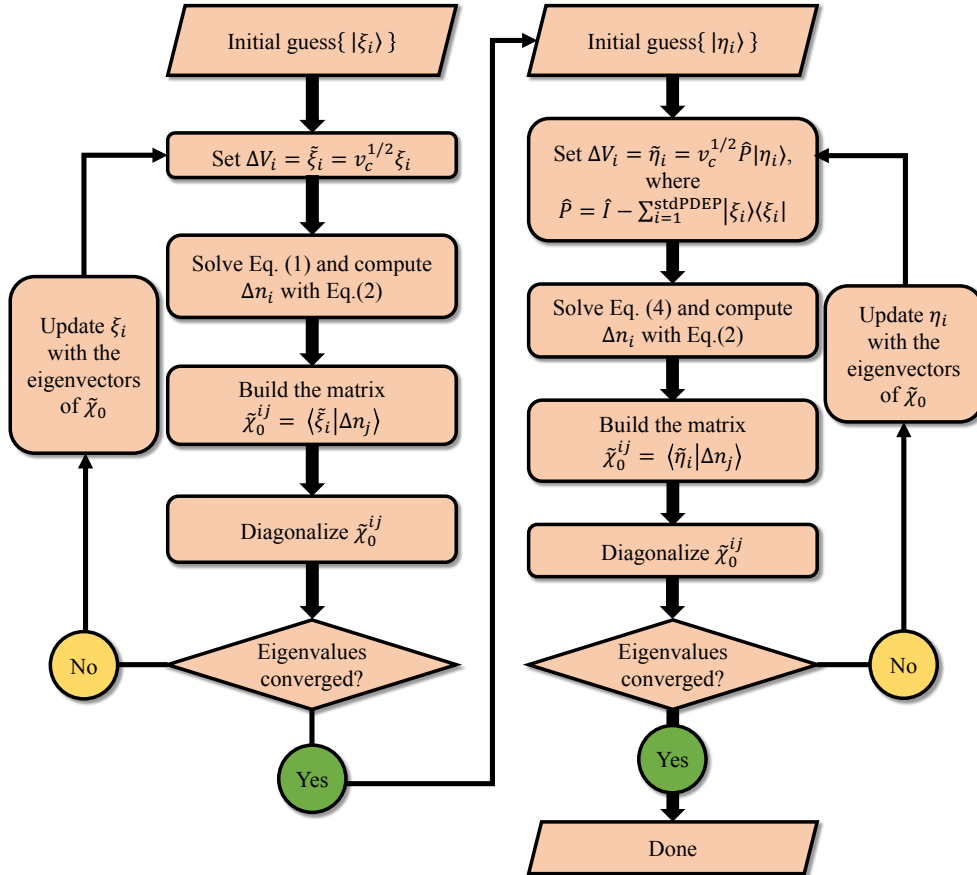


FIG. 2. The workflow used in this work to generate eigenvectors of the dielectric matrix using the Kohn-Sham Hamiltonian (stdPDEP) and using the kinetic operator (kinPDEP). See text.

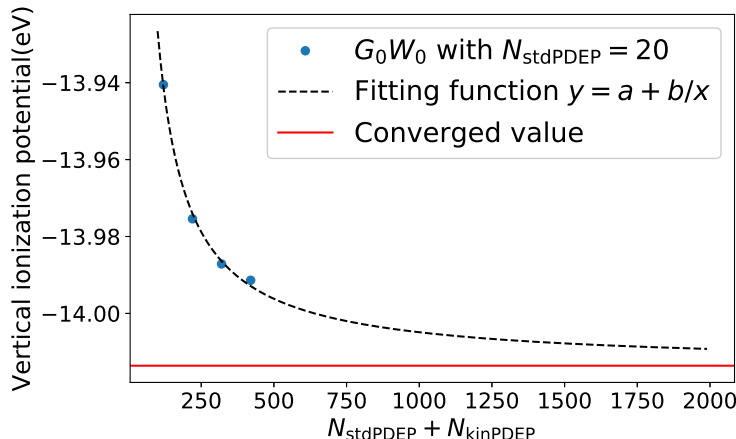


FIG. 3. Extrapolation of G_0W_0 energy of highest occupied orbital of methane with respect to total number of eigenpotential used ($N_{\text{stdPDEP}} + N_{\text{kinPDEP}}$). In this plot, $N_{\text{stdPDEP}} = 20$ and $N_{\text{kinPDEP}} = 100, 200, 300, 400$ for the four points, respectively.

TABLE I. Vertical ionization potential (eV) obtained at the G_0W_0 @PBE level of theory with different numbers of standard and kinetic PDEPs. (A) 20 stdPDEPs + up to 400 kinPDEPs and extrapolated; (B) 100 stdPDEPs + up to 400 kinPDEPs and extrapolated; (C) pure stdPDEPs and extrapolated. A detailed discussion of extrapolations of quasiparticle energies can be found in Ref. 9. See also Fig. 3 of the SI.

Molecule	A	B	C
C_2H_2	11.07	11.06	11.06
C_2H_4	10.41	10.40	10.40
$\text{C}_4\text{H}_4\text{S}$	8.80	8.77	8.76
C_6H_6	9.17	9.14	9.13
CH_3Cl	11.28	11.26	11.25
CH_3OH	10.58	10.56	10.56
CH_3SH	9.39	9.36	9.36
CH_4	14.01	14.01	14.01
Cl_2	11.51	11.51	11.50
ClF	12.55	12.55	12.54
CO	13.51	13.50	13.50
CO_2	13.32	13.31	13.31
CS	11.00	10.98	10.98
F_2	14.99	14.97	14.97
H_2CO	10.43	10.42	10.42
H_2O	11.82	11.82	11.81
H_2O_2	10.87	10.87	10.86
HCl	12.50	12.50	12.50
HCN	13.20	13.20	13.20
Na_2	4.95	4.95	4.95

from those computed with standard eigenpotentials (extrapolated up to $N_{\text{stdPDEP}} = 2000$).

The two sets of calculations starting with $N_{\text{stdPDEP}} = 100$ and $N_{\text{kinPDEP}} = 200$ amounted to savings of 32% and 15%, respectively.

We now turn to a more complex system, amorphous silicon nitride interfaced with a silicon surface ($\text{Si}_3\text{N}_4/\text{Si}(100)$), whose structure was taken from Ref. 46 (See Fig. 4). This interface is representative of a heterogeneous, low dimensional system.

We computed band offsets (BO) by employing two different methods. The first one is based on the calculation of the local density of electronic states (LDOS);^{46,47} the second one is based on the calculation of the average electrostatic potential which is then used to set a common zero of energy on the two parts of the slab representing the two solids interfaced

TABLE II. Vertical electron affinity (eV) obtained at the G_0W_0 @PBE level of theory with different numbers of standard and kinetic PDEPs. (A) 20 stdPDEPs + up to 400 kinPDEPs and extrapolated; (B) 100 stdPDEPs + up to 400 kinPDEPs and extrapolated; (C) pure stdPDEPs and extrapolated. A detailed discussion of extrapolations of quasiparticle energies can be found in Ref. 9. See also Figure 3 of the SI.

Molecule	A	B	C
C_2H_2	-2.42	-2.41	-2.41
C_2H_4	-1.75	-1.75	-1.75
$\text{C}_4\text{H}_4\text{S}$	-0.85	-0.81	-0.80
C_6H_6	-1.01	-0.96	-0.96
CH_3Cl	-1.17	-1.16	-1.16
CH_3OH	-0.89	-0.89	-0.89
CH_3SH	-0.88	-0.88	-0.88
CH_4	-0.64	-0.64	-0.64
Cl_2	1.65	1.64	1.65
ClF	1.28	1.28	1.28
CO	-1.56	-1.57	-1.57
CO_2	-0.97	-0.97	-0.97
CS	0.49	0.51	0.51
F_2	1.16	1.16	1.16
H_2CO	-0.69	-0.68	-0.68
H_2O	-0.90	-0.90	-0.90
H_2O_2	-1.80	-1.79	-1.79
HCl	-1.07	-1.07	-1.07
HCN	-2.08	-2.08	-2.08
Na_2	0.64	0.63	0.63

TABLE III. Quasiparticle energies (eV) of C_{60} calculated at the G_0W_0 @PBE level of theory. Energy levels are labeled by their symmetry in point group I_h . $N_{\text{stdPDEP}} = 100$ and $N_{\text{stdPDEP}} = 200$ are calculations with 100 and 200 stdPDEPs and up to 400 kinPDEPs and extrapolated. $N_{\text{kinPDEP}} = 0$ is the calculation with pure stdPDEPs and extrapolated. (See text)

Energy levels	$N_{\text{stdPDEP}} = 100$	$N_{\text{stdPDEP}} = 200$	$N_{\text{kinPDEP}} = 0$	G_0W_0	Expt
t_{1g}	-1.70	-1.66	-1.70		
t_{1u}	-2.70	-2.77	-2.82	-2.74 ^a , -2.62 ^b , -2.82 ^c	-2.69 ^d
h_u	-7.32	-7.32	-7.38	-7.31 ^a , -7.21 ^b , -7.37 ^c	-7.61 ^d , -7.6 ^e
$g_g + h_g$	-8.46, -8.52	-8.46, -8.51	-8.51, -8.56	-8.68 ^c , -8.69 ^c	-8.59 ^e

^a Ref. 27: with 700 standard eigenpotentials;

^b Ref. 20: with 27387 SAPOs, where SAPO stands for simple approximate physical orbitals;

^c Ref. 43: plane wave energy cutoff of 45 Ry and cell edge of 31.7 bohr;

^d Ref. 44;

^e Ref. 45.

with each other.⁴⁸ The average electrostatic potential was fitted with the method proposed in Ref. 49. We used a plane wave energy cutoff of 70 Ry. We also performed G_0W_0 @PBE calculations for each bulk system separately and obtained quasiparticle energies.

The local density of states is given by:

$$D(\varepsilon, z) = 2 \sum_i \int \frac{dx}{L_x} \int \frac{dy}{L_y} |\psi_i(x, y, z)|^2 \delta(\varepsilon - \varepsilon_i), \quad (6)$$

where z is the direction perpendicular to the interface, $\psi_i(x, y, z)$ is the wavefunction, the factor 2 represents spin degeneracy. We computed the variation of the valence band maximum(VBM) and conduction band minimum(CBM) as a function of the direction (z) perpendicular to the interface⁴⁶

$$\int_{\text{VBM}}^{E_F} D(\varepsilon, z) d\varepsilon = \int_{E_F}^{\text{CBM}} D(\varepsilon, z) d\varepsilon = \Delta \int_{-\infty}^{E_F} D(\varepsilon, z) d\varepsilon \quad (7)$$

where E_F is the Fermi energy and Δ is a constant that is chosen to be 0.003.⁴⁶ We follow a common procedure adopted to describe the electronic structure of interfaces described in Ref. 46 and 47. The band offsets (see Table V) at the PBE level of theory were determined to be 0.83 eV and 1.49 eV for the valence band and conduction band, respectively, which are in agreement with the results of 0.8 eV and 1.5 eV reported in Ref. 46.

As mentioned above, another method to obtain the valence band offset (VBO) and conduction band offset (CBO) is to align energy levels with respect to electrostatic potentials. Following Ref. 49, the electrostatic potential was computed as:

$$\bar{V}(\mathbf{r}) = V_H(\mathbf{r}) + V_{\text{loc}}(\mathbf{r}) - \sum_i \bar{V}_{\text{at}}^{(i)}(|\mathbf{r} - \mathbf{r}_i|) \quad (8)$$

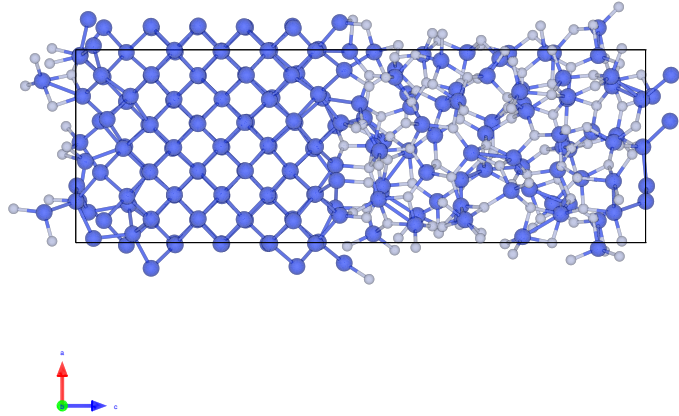


FIG. 4. Ball and stick representation of the atomistic structure⁴⁶ of the $\text{Si}_3\text{N}_4/\text{Si}(100)$ interface used in our study.

where $\bar{V}_{\text{at}}^{(i)}$ is the potential near the core region obtained from neutral atom calculations.

With this method, VBO and CBO at the PBE level are found to be 0.89 eV and 1.63 eV.

To compute G_0W_0 corrections on band offsets, we performed $G_0W_0@\text{PBE}$ calculations of bulk silicon and amorphous silicon nitride. In Table IV, quasiparticle corrections to Kohn-Sham energies of bulk silicon and amorphous silicon nitride are shown. The second and third columns are computed with 1000 and 2000 standard eigenpotentials. The fitted G_0W_0 reference results are extrapolated with 500, 1000, 1500 and 2000 standard eigenpotentials. To test accuracy of kinetic eigenpotentials, we started with 400 stdPDEPs and added 100, 200, 300, 400 kinPDEPs, after which the same extrapolation was applied. We calculated VBO and CBO at the G_0W_0 level by applying quasiparticle corrections on PBE results. After applying quasiparticle corrections on LDOS results, VBO and CBO are 1.41 eV and 1.88 eV while the VBO and CBO are found to be 1.46 eV and 2.02 eV after applying corrections to results based on electrostatic potential alignment. Both of them are close to the range of

TABLE IV. Quasiparticle energies of valence band maximum (VBM) and conduction band minimum (CBM) of bulk silicon and amorphous Si_3N_4 computed with standard eigenpotentials and by combining standard and kinetic eigenpotentials. Columns $N_{\text{stdPDEP}} = 1000$ and $N_{\text{stdPDEP}} = 2000$ are calculations done with 1000 and 2000 stdPDEPs; column Fit is extrapolated results; column $N_{\text{kinPDEP}} = 400$ is calculation with up to 400 kinPDEPs and extrapolated. (See text)

	$N_{\text{stdPDEP}} = 1000$	$N_{\text{stdPDEP}} = 2000$	Fit	$N_{\text{kinPDEP}} = 400$
Si VBM	5.70	5.55	5.45	5.53
Si CBM	7.03	6.91	6.79	6.82
$a - \text{Si}_3\text{N}_4$ VBM	7.14	7.01	7.01	6.99
$a - \text{Si}_3\text{N}_4$ CBM	11.99	11.87	11.83	11.83

TABLE V. Band gaps of bulk Si, $a - \text{Si}_3\text{N}_4$, and band offsets (VBO&CBO) of the interface.(see Fig. 4) All values are in eV.

Method \ Energy	VBO	CBO	E_g^{Si}	$E_g^{\text{Si}_3\text{N}_4}$
LDOS Potential	0.83	1.49	0.67	3.19
	0.89	1.63	0.76	3.19
	0.8	1.5	0.7	3.17
G_0W_0 Potential	1.41	1.88	1.29	4.77
	1.46	2.02	1.29	4.77
	1.5	1.9	1.3	4.87
Expt	1.5-1.78 ^b	1.82-2.83 ^c	1.17 ^d	4.5-5.5 ^e

^a Ref. 46;

^b Ref. 50-52;

^c Estimated by the other three experimental values;

^d Ref. 53;

^e Ref. 54-56.

experimental results of 1.5 – 1.78 eV and 1.82 – 2.83 eV. Time saving when using kinetic eigenpotentials to obtain quasiparticle corrections was approximately $\sim 50\%$.

IV. CONCLUSION

The method introduced in Ref. 9,26–28 to compute quasiparticle energies using the G_0W_0 approximation avoids the calculation of virtual electronic states and the inversion and storage of large dielectric matrices, thus leading to substantial computational savings. Building on

the strategy proposed in Ref.^{24,25} and implemented in the WEST code,²⁸ here we proposed an approximation of the spectral decomposition of dielectric matrices that further improve the efficiency of G_0W_0 calculations. In particular we built sets of eigenpotentials used as a basis to expand the Green function and the screened Coulomb interaction by solving two separate Sternheimer equations: one using the Hamiltonian of the system, to obtain the eigenvectors corresponding to the lowest eigenvalues of the response function, and one equation using just the kinetic energy operator to obtain the eigenpotentials corresponding to higher eigenvalues. We showed that without compromising much accuracy, this approximation reduces the cost of G_0W_0 calculations by 10%-50%, depending on the system, with the most savings observed for the largest systems studied here.

ACKNOWLEDGMENTS

We thank He Ma, Ryan L. McAvoy and Ngoc Linh Nguyen for useful discussions. This work was supported by MICCoM, as part of the Computational Materials Sciences Program funded by the U.S. Department of Energy, Office of Science, Basic Energy Sciences, Materials Sciences and Engineering Division through Argonne National Laboratory, under contract number DE-AC02-06CH11357. This research used resources of the Argonne Leadership Computing Facility, which is a DOE Office of Science User Facility supported under Contract DE-AC02-06CH11357, and resources of the University of Chicago Research Computing Center.

REFERENCES

- ¹P. Hohenberg and W. Kohn, “Inhomogeneous electron gas,” Physical Review **136**, B864 (1964).
- ²W. Kohn and L. J. Sham, “Self-consistent equations including exchange and correlation effects,” Physical Review **140**, A1133 (1965).
- ³R. M. Martin, *Electronic structure: basic theory and practical methods* (Cambridge University Press, 2004).
- ⁴G. Onida, L. Reining, and A. Rubio, “Electronic excitations: density-functional versus many-body green’s-function approaches,” Review of Modern Physics **74**, 601–659 (2002).
- ⁵R. M. Martin, L. Reining, and D. M. Ceperley, *Interacting electrons* (Cambridge University Press, 2016).
- ⁶L. Hedin, “New method for calculating the one-particle green’s function with application to the electron-gas problem,” Physical Review **139**, A796 (1965).
- ⁷M. J. van Setten, F. Caruso, S. Sharifzadeh, X. Ren, M. Scheffler, F. Liu, J. Lischner, L. Lin, J. R. Deslippe, S. G. Louie, *et al.*, “GW 100: Benchmarking G_0W_0 for molecular systems,” Journal of Chemical Theory and Computation **11**, 5665–5687 (2015).
- ⁸E. Maggio, P. Liu, M. J. van Setten, and G. Kresse, “GW 100: a plane wave perspective for small molecules,” Journal of Chemical Theory and Computation **13**, 635–648 (2017).
- ⁹M. Govoni and G. Galli, “GW100: Comparison of methods and accuracy of results obtained with the west code,” Journal of Chemical Theory and Computation **14**, 1895–1909 (2018).
- ¹⁰P. Scherpelz, M. Govoni, I. Hamada, and G. Galli, “Implementation and validation of fully relativistic gw calculations: spin–orbit coupling in molecules, nanocrystals, and solids,”

Journal of Chemical Theory and Computation **12**, 3523–3544 (2016).

¹¹N. P. Brawand, M. Vörös, M. Govoni, and G. Galli, “Generalization of dielectric-dependent hybrid functionals to finite systems,” Physical Review X **6**, 041002 (2016).

¹²D. Golze, M. Dvorak, and P. Rinke, “The GW compendium: A practical guide to theoretical photoemission spectroscopy,” Frontiers in chemistry **7** (2019).

¹³M. S. Hybertsen and S. G. Louie, “First-principles theory of quasiparticles: calculation of band gaps in semiconductors and insulators,” Physical Review Letters **55**, 1418 (1985).

¹⁴M. S. Hybertsen and S. G. Louie, “Electron correlation and the band gap in ionic crystals,” Physical Review B **32**, 7005–7008 (1985).

¹⁵M. S. Hybertsen and S. G. Louie, “Electron correlation in semiconductors and insulators: Band gaps and quasiparticle energies,” Physical Review B **34**, 5390 (1986).

¹⁶G. Strinati, H. Mattausch, and W. Hanke, “Dynamical correlation effects on the quasiparticle bloch states of a covalent crystal,” Physical Review Letters **45**, 290 (1980).

¹⁷G. Strinati, H. Mattausch, and W. Hanke, “Dynamical aspects of correlation corrections in a covalent crystal,” Physical Review B **25**, 2867 (1982).

¹⁸S. L. Adler, “Quantum theory of the dielectric constant in real solids,” Physical Review **126**, 413 (1962).

¹⁹N. Wiser, “Dielectric constant with local field effects included,” Physical Review **129**, 62 (1963).

²⁰G. Samsonidze, M. Jain, J. Deslippe, M. L. Cohen, and S. G. Louie, “Simple approximate physical orbitals for GW quasiparticle calculations,” Physical Review Letters **107**, 186404 (2011).

²¹F. Bruneval and X. Gonze, “Accurate *gw* self-energies in a plane-wave basis using only a few empty states: Towards large systems,” Phys. Rev. B **78**, 085125 (2008).

²²W. Gao, W. Xia, X. Gao, and P. Zhang, “Speeding up *gw* calculations to meet the challenge of large scale quasiparticle predictions,” *Scientific reports* **6**, 36849 (2016).

²³J. Soininen, J. Rehr, and E. L. Shirley, “Electron self-energy calculation using a general multi-pole approximation,” *Journal of Physics: Condensed Matter* **15**, 2573 (2003).

²⁴H. F. Wilson, F. Gygi, and G. Galli, “Efficient iterative method for calculations of dielectric matrices,” *Physical Review B* **78**, 113303 (2008).

²⁵H. F. Wilson, D. Lu, F. Gygi, and G. Galli, “Iterative calculations of dielectric eigenvalue spectra,” *Physical Review B* **79**, 245106 (2009).

²⁶H.-V. Nguyen, T. A. Pham, D. Rocca, and G. Galli, “Improving accuracy and efficiency of calculations of photoemission spectra within the many-body perturbation theory,” *Phys. Rev. B* **85**, 081101 (2012).

²⁷T. A. Pham, H.-V. Nguyen, D. Rocca, and G. Galli, “GW calculations using the spectral decomposition of the dielectric matrix: Verification, validation, and comparison of methods,” *Physical Review B* **87**, 155148 (2013).

²⁸M. Govoni and G. Galli, “Large scale GW calculations,” *Journal of Chemical Theory and Computation* **11**, 2680–2696 (2015).

²⁹R. Sternheimer, “Electronic polarizabilities of ions from the hartree-fock wave functions,” *Physical Review* **96**, 951 (1954).

³⁰S. Baroni, S. De Gironcoli, A. Dal Corso, and P. Giannozzi, “Phonons and related crystal properties from density-functional perturbation theory,” *Reviews of Modern Physics* **73**, 515 (2001).

³¹H. Ma, M. Govoni, F. Gygi, and G. Galli, “A finite-field approach for gw calculations beyond the random phase approximation,” *Journal of Chemical Theory and Computation* **15**, 154–164 (2018).

³²D. Lu, F. Gygi, and G. Galli, “Dielectric properties of ice and liquid water from first-principles calculations,” *Physical Review Letters* **100**, 147601 (2008).

³³J. Lindhard, “On the properties of a gas of charged particles,” *Dan. Vid. Selsk Mat.-Fys. Medd.* **28**, 8 (1954).

³⁴D. Rocca, “Random-phase approximation correlation energies from lanczos chains and an optimal basis set: Theory and applications to the benzene dimer,” *The Journal of Chemical Physics* **140**, 18A501 (2014).

³⁵D. Lu, Y. Li, D. Rocca, and G. Galli, “Ab initio calculation of van der waals bonded molecular crystals,” *Physical Review Letters* **102**, 206411 (2009).

³⁶P. Giannozzi, S. Baroni, N. Bonini, M. Calandra, R. Car, C. Cavazzoni, D. Ceresoli, G. L. Chiarotti, M. Cococcioni, I. Dabo, *et al.*, “Quantum espresso: a modular and open-source software project for quantum simulations of materials,” *Journal of Physics: Condensed Matter* **21**, 395502 (2009).

³⁷P. Giannozzi, O. Andreussi, T. Brumme, O. Bunau, M. B. Nardelli, M. Calandra, R. Car, C. Cavazzoni, D. Ceresoli, M. Cococcioni, N. Colonna, I. Carnimeo, A. D. Corso, S. de Gironcoli, P. Delugas, R. A. DiStasio, A. Ferretti, A. Floris, G. Fratesi, G. Fugallo, R. Gebauer, U. Gerstmann, F. Giustino, T. Gorni, J. Jia, M. Kawamura, H.-Y. Ko, A. Kokalj, E. Küçükbenli, M. Lazzeri, M. Marsili, N. Marzari, F. Mauri, N. L. Nguyen, H.-V. Nguyen, A. O. de-la Roza, L. Paulatto, S. Poncé, D. Rocca, R. Sabatini, B. Santra, M. Schlipf, A. P. Seitsonen, A. Smogunov, I. Timrov, T. Thonhauser, P. Umari, N. Vast, X. Wu, and S. Baroni, “Advanced capabilities for materials modelling with quantum ESPRESSO,” *Journal of Physics: Condensed Matter* **29**, 465901 (2017).

³⁸J. P. Perdew, K. Burke, and M. Ernzerhof, “Generalized gradient approximation made simple,” *Physical Review Letters* **77**, 3865–3868 (1996).

³⁹M. Schlipf and F. Gygi, “Optimization algorithm for the generation of oncv pseudopotentials,” Computer Physics Communications **196**, 36–44 (2015).

⁴⁰D. Hamann, “Optimized norm-conserving vanderbilt pseudopotentials,” Physical Review B **88**, 085117 (2013).

⁴¹L. A. Curtiss, P. C. Redfern, K. Raghavachari, and J. A. Pople, “Assessment of gaussian-2 and density functional theories for the computation of ionization potentials and electron affinities,” The Journal of Chemical Physics **109**, 42–55 (1998).

⁴²E. R. D. J. III, NIST Computational Chemistry Comparison and Benchmark Database, NIST Standard Reference Database Number 101, Release 18 (October 2016).

⁴³X. Qian, P. Umari, and N. Marzari, “First-principles investigation of organic photovoltaic materials C₆₀, C₇₀,[C₆₀]pcbm, and bis-[C₆₀]pcbm using a many-body G₀W₀-lanczos approach,” Physical Review B **91**, 245105 (2015).

⁴⁴E. P. Linstrom and W. Mallard, NIST Chemistry WebBook, NIST Standard Reference Database Number 69, National Institute of Standards and Technology, Gaithersburg MD, 20899.

⁴⁵D. L. Lichtenberger, K. W. Nebesny, C. D. Ray, D. R. Huffman, and L. D. Lamb, “Valence and core photoelectron spectroscopy of C₆₀, buckminsterfullerene,” Chemical Physics Letters **176**, 203–208 (1991).

⁴⁶T. Anh Pham, T. Li, H.-V. Nguyen, S. Shankar, F. Gygi, and G. Galli, “Band offsets and dielectric properties of the amorphous Si₃N₄/Si(100) interface: A first-principles study,” Applied Physics Letters **102**, 241603 (2013).

⁴⁷T. Yamasaki, C. Kaneta, T. Uchiyama, T. Uda, and K. Terakura, “Geometric and electronic structures of SiO₂/Si(001) interfaces,” Physical Review B **63**, 115314 (2001).

⁴⁸C. G. Van de Walle and R. M. Martin, “Theoretical study of band offsets at semiconductor interfaces,” Physical Review B **35**, 8154–8165 (1987).

⁴⁹R. Sundararaman and Y. Ping, “First-principles electrostatic potentials for reliable alignment at interfaces and defects,” The Journal of Chemical Physics **146**, 104109 (2017).

⁵⁰J. W. Keister, J. E. Rowe, J. J. Kolodziej, H. Niimi, T. E. Madey, and G. Lucovsky, “Band offsets for ultrathin SiO₂ and Si₃N₄ films on Si(111) and Si(100) from photoemission spectroscopy,” Journal of Vacuum Science & Technology B: Microelectronics and Nanometer Structures Processing, Measurement, and Phenomena **17**, 1831–1835 (1999).

⁵¹V. A. Gritsenko, A. V. Shaposhnikov, W. Kwok, H. Wong, and G. M. Jidomirov, “Valence band offset at silicon/silicon nitride and silicon nitride/silicon oxide interfaces,” Thin Solid Films **437**, 135–139 (2003).

⁵²M. Higuchi, S. Sugawa, E. Ikenaga, J. Ushio, H. Nohira, T. Maruizumi, A. Teramoto, T. Ohmi, and T. Hattori, “Subnitride and valence band offset at Si₃N₄/Si interface formed using nitrogen-hydrogen radicals,” Applied Physics Letters **90**, 123114 (2007).

⁵³C. Kittel, *Introduction to solid state physics* (Wiley, 2005).

⁵⁴A. M. Goodman, “Photoemission of electrons and holes into silicon nitride,” Applied Physics Letters **13**, 275–277 (1968).

⁵⁵J. Bauer, “Optical properties, band gap, and surface roughness of Si₃N₄,” Physica Status Solidi (a) **39**, 411–418 (1977).

⁵⁶S. V. Deshpande, E. Gulari, S. W. Brown, and S. C. Rand, “Optical properties of silicon nitride films deposited by hot filament chemical vapor deposition,” Journal of Applied Physics **77**, 6534–6541 (1995).